in agreement with the chemical evidence.

The preceding discussion implies that orbital overlap is an important criterion for determining the strength of the chemisorption bond and that the nature of the orbital in an adsorbing molecule which is preferred by the surface can be substantially altered by modifying the surface composition. In fact, the initial chemisorption experiments reported for the oxygen pretreated molybdenum surface suggest that adsorption selectivity for molecular Lewis bases is controlled by the geometric structure of the electronic states at the surface.[65,68] It remains to be shown whether surface composition modifiers less electronegative than oxygen will produce similar adsorption selectivity as well as whether it can be produced with other metals. It will also be important to investigate adsorption selectivity with molecular Lewis acids and with molecular Lewis bases other than nitrogen bases and π-electron donors in order to evaluate the generality of the overlap criterion.

VII. Summary and Conclusion

The concept of Lewis acids and bases was briefly reviewed. The dependence of base-strength ordering on the nature of the reference acid was demonstrated for both the solution phase and gas phase environments. By adapting the equations of perturbational molecular orbital theory to the gas phase environment, we showed that a reversal in base-strength ordering must be due to changes in the orbital overlap of the electron donor with the electron acceptor. This was seen to be a consequence of the principle of maximum orbital overlap.

The classification of surface–adsorbate interactions as acid–base was established by using the sign of the work-function change which accompanies simple adsorption. The surface acid–base adduct was shown to exhibit an inductive effect similar to that seen in molecules. The production of localized Lewis acid sites was demonstrated for oxygen-incorporation structures on Mo(100) and Ni(110) by using chemical evidence as well as measurements of the surface polarizability.

The most interesting conclusion from this discussion is that the spatial extent of electronic states at the surface, that is whether they are delocalized over two or more surface atoms or localized mainly on a single surface atom, may be the determining factor in adsorption and surface chemical reaction selectivity. In essence, the description of surface electronic structures as localized or delocalized is merely a supplementary classification scheme on top of the primary classification as acid or base. It may serve to provide both qualitative predictions and rationalizations of a wide variety of surface chemical phenomena in the same way that the classifications "hard and soft" have provided for a qualitative understanding of solution phase Lewis acid–base chemistry.

Acknowledgment. We gratefully acknowledge the support of the National Science Foundation under Grant No. CHE-7909268.

Appendix I. Calculation of the Second Ionization Potential

The production of a doubly ionized molecule can be decomposed into two steps:

$$M \rightarrow M^+(C) + e^- \quad (A1)$$

$$M^+(C) \rightarrow M^{2+}(VV) + e^- \quad (A2)$$

The notations $M^+(C)$ and $M^{2+}(VV)$ indicate that the hole or holes are located in a core level, C, or in valence orbitals, VV. The free electrons are to be considered at rest at infinite separation from the positive ion. The energy associated with (A1) is just the core level binding energy for the gas phase molecule measured by X-ray photoelectron spectroscopy, BE(C). The energy of (A2) is just the negative of the Auger electron kinetic energy arising from the (CVV) Auger process, -KE(CVV). For the case where the doubly ionized cation, $M^{2+}(VV)$, is equivalent to the cation produced by removing the two highest-energy electrons from neutral M, the second ionization potential can be written:

$$IP_2 = BE(C) - KE(CVV) - IP_1 \quad (A3)$$

where IP_1 is the first ionization potential.

Registry No. $CH_3CH_2NH_2$, 75-04-7; $CH_3(CH_2)_2NH_2$, 107-10-8; $CH_3(CH_2)_3NH_2$, 109-73-9; $CF_3CH_2NH_2$, 753-90-2; $CF_3(CH_2)_2NH_2$, 460-39-9; $CF_3(CH_2)_3NH_2$, 819-46-5; H_2O, 7732-18-5; CH_3OH, 67-56-1; CH_3CN, 75-05-8; CH_3OCH_3, 115-10-6; NH_3, 7664-41-7; C_2H_4, 74-85-1; C_6H_6, 71-43-2.

Atom–Atom Potential Analysis of the Packing Characteristics of Carboxylic Acids. A Study Based on Experimental Electron Density Distributions

Z. Berkovitch-Yellin* and L. Leiserowitz*

Contribution from the Department of Structural Chemistry, The Weizmann Institute of Science, Rehovot 76100, Israel. *Received October 26, 1981*

Abstract: Information contained in electron density distributions, derived from X-ray diffraction data, was exploited to improve the electrostatic parameters of atom–atom potential functions of the carboxyl group and thus to obtain a better estimate of the Coulomb intermolecular energies. The proton affinities of the carbonyl oxygen atom of the amide and carboxyl groups were compared in terms of electrostatic potential energy around these atoms and correlated with hydrogen-bonding properties. Energy calculations were undertaken to account for various characteristic packing motifs of carboxylic acid molecules, including the geometry of the catemer motif, order–disorder of the carboxyl dimer, preferred stacking of carboxyl dimers, the role played by C–H···O(carbonyl) interactions in stabilizing overall packing, characteristic packing of substituted benzoic acids, and the stability of the observed crystal structures of oxalic acid and formic acid, via the generation and analysis of ensembles of alternative crystal structures.

1. Introduction

In a previous paper we demonstrated the role played by intermolecular Coulomb potentials in determining the molecular packing modes of amides in the crystal;[1] the atomic electrostatic properties used in that study were derived from low-temperature X-ray diffraction data. The aim of the present work is to account in a similar manner for some of the characteristic molecular packing modes of carboxylic acids.

Crystal packing of carboxylic acids has been studied in terms of atom–atom potentials by several groups, notably Derissen and Smit[2] and Hagler and Lifson.[3] The latter derived a force field

(1) Z. Berkovitch-Yellin and L. Leiserowitz, *J. Am. Chem. Soc.*, **102**, 7677 (1980).

0002-7863/82/1504-4052$01.25/0

for carboxylic acids which they applied to a variety of crystal structures. Our approach in this study is different: We have modified the electrostatic term of the energy functions by adding to the atomic charges, which are commonly used, atomic dipoles and quadrupole moments, which allow a better description of the asymmetric charge distribution around each atomic center. Moreover, the electrostatic properties of the carboxyl group were derived from experimental density maps. We placed emphasis on characteristic packing motifs rather than complete crystal packing. This approach also allowed us, in several cases, to construct from a given one- or two-dimensional hydrogen-bonding motif several different three-dimensional arrangements and to compare their lattice energies with those of the observed crystal structures.[4]

2. Parameters for the Energy Calculations

The intermolecular potential energy for a pair of atoms i and j separated by a distance r_{ij} can be represented in the form

$$V(r) = -Ar_{ij}^{-6} + Br_{ij}^{-9} + \int \frac{\rho_i(r)\rho_j(r)\ dv_i\ dv_j}{r_{ij}}$$

The first two terms are van der Waals interactions, the third term is the Coulomb energy, where $\rho_i(r)$ and $\rho_j(r)$ are the atomic charge distributions, and r is measured from the nucleus. It is convenient to work with the atomic deformation density $\delta\rho(r)$, which is the electron density of the bonded atom minus that of the free atom.[6] The Coulomb energy for nonoverlapping atoms is given then by

$$\int \frac{\delta\rho_i(r)\delta\rho_j(r)\ dv_i\ dv_j}{r_{ij}}$$

This integral can be evaluated via the multipole moments[7] of $\delta\rho(r)$. As was demonstrated in a previous paper,[1] it is sufficient to employ only the first three moments, namely, the atomic net charge, the atomic dipole moment, and the quadrupole moment.

2.1. Electrostatic Parameters. The electrostatic properties of the carboxyl group were derived from the experimental electron density distributions of the complex allenedicarboxylic acid–acetamide[8] and 1,3-diethylbicyclobutane-*exo*, *exo*-2,4-dicarboxylic acid,[9] using the atomic partitioning scheme introduced by Hirshfeld.[6] Excellent agreement was found between the electrostatic parameters of the carboxyl group as derived from the experimental density maps and from a theoretical map of formic acid.[10] The atomic net charges, dipole moments, and quadrupole moments of the carboxyl group used in this study are given in Table I. For calculations involving various carboxylic acid molecules, we have made use of electrostatic parameters of other atomic types. In all cases the parameters, but for those of the aromatic C–H group, were derived from experimental densities.

2.2. van der Waals Parameters. The van der Waals parameters for C, O, and H were those of Lifson, Hagler, and co-workers,[3] which were slightly modified. In deriving their force field for carboxylic acids, Lifson and Hagler assumed that the carbonyl oxygen atoms of the amide and carboxyl groups are similar in nature and were thus assigned identical parameters. However, we found distinct differences between these two different oxygen atoms, which will be elaborated upon in section 4. We made slight modifications to the van der Waals parameters of the oxygen atom and of the hydroxy hydrogen atom. This was done ad hoc on the basis of the following considerations: We adjusted the parameters to yield an energy minimum for a formic acid cyclic dimer (**1**) with an O–H···O distance of 2.65 Å and to yield motif **2** with an interdimer O(hydroxyl)···O(hydroxyl) distance of 3.0 Å, which are the average observed distances for several structures.[11]

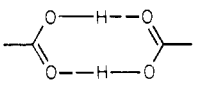

1

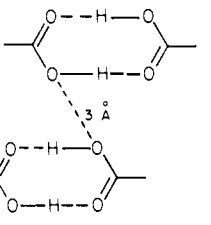

2

We assumed here that the van der Waals parameters of the carbonyl and hydroxyl oxygen atoms are identical because of the strong correlation between their parameters in dimer **1**. We checked the modified parameters by computing the crystal energies of formic and acetic acids. The values obtained, −15.2 and −15.6 kcal/mol, respectively, are in excellent agreement with the reported corresponding experimental values[3] of −15.2 and −16.3 kcal/mol.

Table I. Electrostatic Properties and van der Waals Potential Parameters

a. Net Atomic Charges (×10⁴) and Dipole and Second Moments (×10⁴) of the Carboxyl Group in Local Coordinate System x, y, z Centered on Each Atom

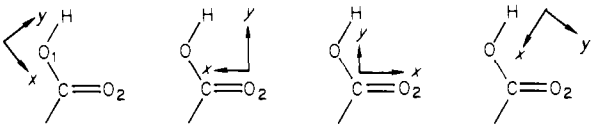

atom	atom charge,[a] e	dipole moment,[a] e Å			second moment,[a] e Å²					
		d_x	d_y	d_z	μ_{xx}	μ_{yy}	μ_{zz}	μ_{xy}	μ_{yz}	μ_{xz}
O_1	−1393	71	738	0	560	363	644	−334	0	0
O_2	−2214	19	235	0	9	298	393	−137	0	0
C	1839	−306	215	0	721	1029	2478	−38	0	0
H(O)	1493	−306	−121	0	191	765	891	−28	0	0

b. van der Waals Potential Parameters A and B[b]

atom pair	A, kcal/mol	B, kcal/mol
C–C	355.0	12500.0
O–O	1410.0	45800.0
H(C)–H(C)	15.0	445.0
H(O)–H(O)	2.9	0.0
O–C	707.5	23927.0
H(C)–C	73.0	2358.5
H(C)–O	145.4	4514.5
H(O)–C	32.1	0.0
H(O)–O	63.6	0.0
H(O)–H(C)	6.6	0.0

[a] The net charge for atom i, $q_i = -\int \delta\rho_i(r)\ dv$, where $\delta\rho_i(r)$ is the atom deformation density and r is measured from the nucleus of atom i; the negative sign obeys the convention that electrons are negatively charged. The atomic dipole moment $d_{i,x} = -\int x\delta\rho(r)\ dv$, where x is the component of vector $\mathbf{r}$. Similar expressions apply to $d_{i,y}$ and $d_{i,z}$. The second moment tensor of $\delta\rho_i(r)$ has six independent components, $\mu_{i,xx}, \mu_{i,yy}, \mu_{i,zz}, \mu_{i,xy}$, etc. $\mu_{i,xy} = -\int xy\delta\rho_i(r)\ dv$. [b] $V = -Ar^{-6} + Br^{-9}$.

(2) J. L. Derissen and P. H. Smit, *Acta Crystallogr., Sect. A*, **A33**, 230 (1977).
(3) A. T. Hagler, P. Dauber, and S. Lifson, *J. Am. Chem. Soc.*, **101**, 5111 (1979), and references therein.
(4) This method has been used successfully to account for the anomalous hydrogen-bonding arrangement of adipamide[5] and to establish why acetic acid forms the catemer motif in preference to the cyclic hydrogen-bonded dimer.[2]
(5) A. T. Hagler and L. Leiserowitz, *J. Am. Chem. Soc.*, **100**, 5879 (1978).
(6) F. L. Hirshfeld, *Theor. Chim. Acta.*, **44**, 129 (1977).
(7) (a) The electrostatic energy of interaction between two electron density distributions represented by two sets of multipoles was calculated according to the Coulomb law. The equations used were derived from an expression describing the potential energy of a charge distribution in an external field.[7b] (b) J. C. Slater and N. H. Frank, "Electromagnetism", McGraw-Hill, New York, 1947, p 227.
(8) Z. Berkovitch-Yellin and L. Leiserowitz, *Acta Crystallogr., Sect. B*, **B33**, 3670 (1977).
(9) M. Eisenstein and F. L. Hirshfeld, *Acta Crystallogr.*, in press.
(10) M. Eisenstein, Ph.D. Thesis, The Feinberg Graduate School, The Weizmann Institute of Science, Rehovot, Israel, Feb 1981.
(11) L. Leiserowitz, *Acta Crystallogr., Sect. B.*, **B32**, 775 (1976).

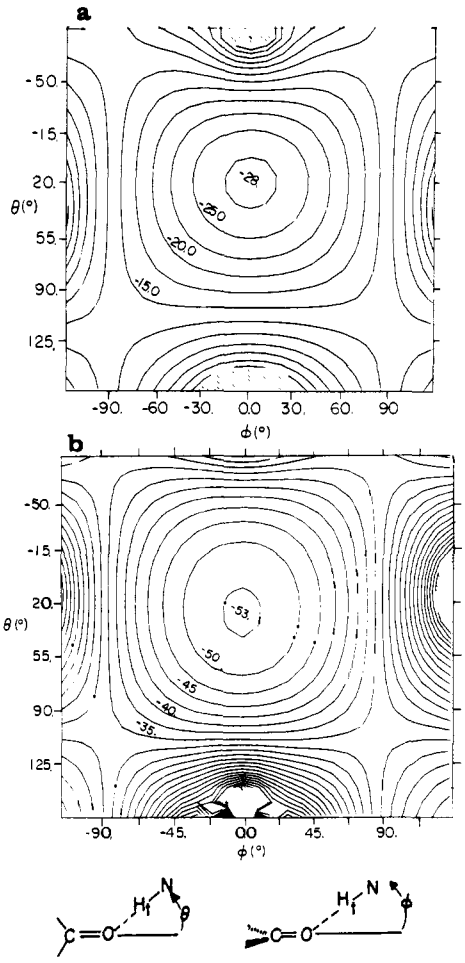

Figure 1. Electrostatic potential energy surface about the carbonyl oxygen atom of (a) formic acid and (b) formamide at a distance R = 1.65 Å. The angles ϕ and θ are defined at the bottom of the figure.

3. Objectives

In this paper we shall make use of these improved parameters. (a) We shall calculate and compare the proton affinities of the carbonyl oxygen atoms of the carboxyl and amide groups in terms of the electrostatic potential energy around these atoms and correlate these affinities with hydrogen-bonding properties of these groups. (b) We shall examine the various ways in which the carboxyl group forms a catemer motif.[12] (c) We shall elucidate the systematic ways in which dimers of carboxylic acids RCO_2H interact with each other in the solid to form the crystal. Here particular attention will be paid to the various distinct stacking motifs of carboxylic dimers in an attempt to interpret the observed order–disorder (O/D) of the carboxyl dimer in energy terms. We shall examine O/D in terms of both inter- and intramolecular interactions and temperature. (d) We shall try to establish quantitatively the role played by CH···O(carboxyl) interactions in determining molecular packing and the conformation of α,β-unsaturated acids. (e) We shall construct various hypothetical three-dimensional arrangements in the crystal structures of α- and β-oxalic acids and of formic acid so as to pinpoint the factors that determine their overall packing.

4. Proton Affinity of the Carboxyl and Amide Oxygen Atoms

There is sufficient evidence from the crystalline state that the carbonyl oxygen atoms of the amide and carboxyl groups have different hydrogen-bonding properties and that the amide oxygen atom is the stronger acceptor of the two;[13] in crystal structures

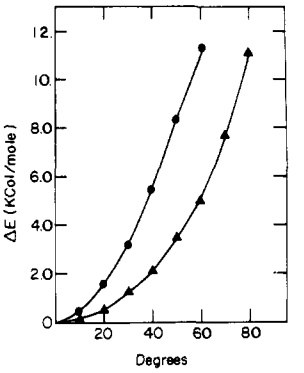

Figure 2. Variation in Coulomb energy ΔE as a function of the angle ϕ (see Figure 1) for the carboxyl group (●) and for the amide group (▲).

where the molecule contains both amide (primary or secondary) and carboxyl groups, as well as in molecular complexes between amides and carboxylic acids, there are cases in which the amide oxygen atom acts as a proton acceptor to both the N–H and O–H proton donors whereas the carboxyl oxygen atom does not participate in any hydrogen bond or forms only one hydrogen bond. The reverse arrangement is very rare. Furthermore, the length of the O–H···O(amide) bond is as short as 2.51 Å in several crystals whereas the O–H···O(carboxyl) bond is generally 2.60–2.65 Å long. Another difference in hydrogen-bond geometry is that the system O—H···O=C(OH)R tends to be coplanar whereas for O—H···O=C(N)R (or N—H···O=C(N)R) systems the pattern of coplanarity does not hold.[13a,14]

We examined the differences in H-bonding properties of these two atoms in terms of Coulomb potentials about the carbonyl oxygen atoms of the amide and acid groups. The calculated Coulomb potential energy for the carbonyl oxygen atom of formic acid is shown in Figure 1a. The potential surface was calculated for a unit positive charge (a proton) placed 1.65 Å from the oxygen atom.[15] This energy surface may be compared with the corresponding surface of formamide (Figure 1b), where the unit positive charge was also placed at 1.65 Å from the oxygen atom.

This comparison (Figure 1) indicates that the amide oxygen atom is a much stronger proton acceptor than the carboxyl oxygen atom. This may be attributed primarily to its greater net charge[1] (−0.39 e vs. −0.22 e). Secondly, the loss of Coulomb energy as a function of the angle ϕ, which corresponds to an out-of-plane approach of the proton donor (Figure 2), is steeper for the carboxyl group than for the amide group. These results are consistent with the observed properties of amide and acids (as mentioned above).

5. Catemer Motif

5.1. Synplanar O=C—OH Conformation. The carboxyl group forms hydrogen-bonded chains via the catemer motif in three more or less distinct arrangements, as shown in **3a–c**.

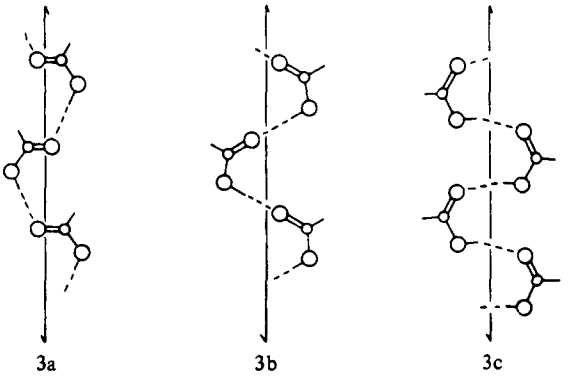

(12) The catemer is a one-dimensional chain in which the carboxyl groups are interlinked by single OH···O bonds.

(13) (a) L. Leiserowitz and F. Nader, *Acta Crystallogr., Sect. B*, **B33**, 2719 (1977). (b) Z. Berkovitch-Yellin, S. Ariel, and L. Leiserowitz, *J. Am. Chem. Soc.*, submitted for publication.

(14) S. Ariel, Ph.D. Thesis, The Feinberg Graduate School, The Weizmann Institute of Science, Rehovot, Israel, 1981.

(15) The position of the unit charge corresponds to the position of the proton donor in an OH···O(carboxyl) bond of 2.65 Å.

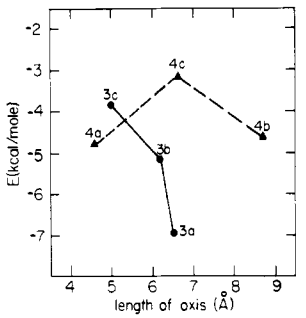

Figure 3. Coulomb energy for various catemer motifs of formic acid in the synplanar and antiplanar conformations: (●) motifs **3a–c** of the synplanar conformer; (▲) motifs **4a–c** of the antiplanar conformer.

In all three arrangements the conformation of O=C—OH is synplanar. There is evidence, based on various packing considerations,[11] that the stability of the catemer decreases upon going from motifs **3a** to **3c**. The Coulomb energies of these three arrangements, keeping the O–H···O bond length at 2.64 Å, is shown in Figure 3.

These calculations definitely demonstrate, on the basis of Coulomb energies, a significant decrease in stabilization energy upon going from motif **3a** to **3c**. Relevant to these calculations is the observation that the motif adopted appears to depend on the nature of the residue R of RCO_2H; motif **3a** requires a nonbulky residue group because of steric factors, so formic,[16] acetic,[17] and tetrolic acids[18] appear in this arrangement. The other motifs, **3b** and **3c**, appear only in enantiomeric crystal structures incorporating chiral molecules. The former (**3b**) appears in the crystal structure of (*R*)-(+)-2,2-diphenyl-1-methylcyclopropanecarboxylic acid[19] and the latter (**3c**) in D-2-methyloctadecanoic acid.[20] Motif **3c** is stabilized by favorable van der Waals interactions between the long apliphatic chains of neighboring molecules along the 5-Å translation axis.

5.2. Antiplanar O=C—OH Conformation. As mentioned above, the carboxyl group in the observed catemer arrangements exhibits the commonly observed synplanar O=C—OH conformation. With the assumption of the alternative antiplanar O=C—OH conformer, three different catemer motifs (**4**) may be constructed.

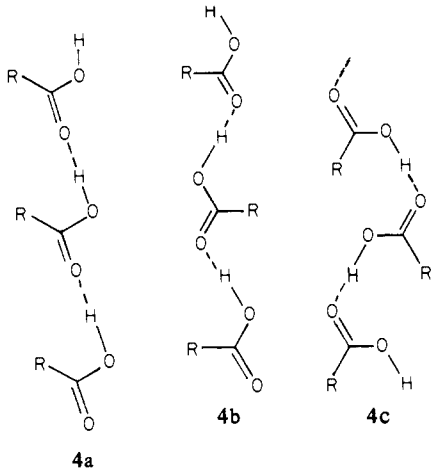

The antiplanar conformation is found, with one exception,[21] only when the carboxylic acid forms an intramolecular O–H···O bond, as shown in **5**.

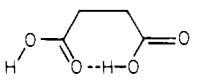

5

According to experimental and theoretical results,[22] the synplanar conformer is at least 2 kcal/mol more stable than the antiplanar conformer. The question then arises whether the hypothetical catemer motifs **4a–c**, incorporating the antiplanar O=C—OH conformer, are precluded because of intramolecular forces only or whether intermolecular forces also play a role here. To clarify this point we examined the Coulomb energies of formic acid with an antiplanar O=C—OH conformation incorporated into the three motifs **4a–c**.[23] The results are shown in Figure 3. These energies are by and large higher than those of motifs **3a–c**, incorporating formic acid in the synplanar arrangement. Consequently, intramolecular, as well as intermolecular, forces favor the synplanar conformer, thus accounting for the absence of motifs **4a–c**.

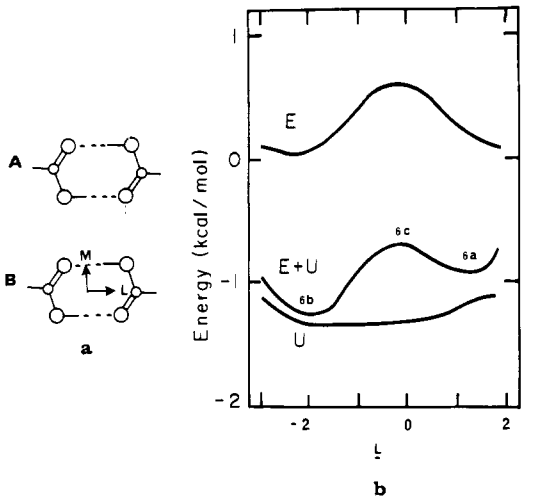

Figure 4. (a) Two coplanar acid dimers related by translation. (b) Energy variation as dimer A is moved relative to dimer B along **L** at m = 5.75 Å. E = Coulomb energy; U = van der Waals energy. The energies of motifs **6a–c** are denoted.

6. Carboxyl Dimers

6.1. Juxtaposition of Coplanar Carboxyl Dimers. Only a handful of carboxylic acid molecules RCO_2H appear in the catemer motif; the majority form cyclic dimers. The dimer affords an advantage over the catemer insofar as its packing properties are not directly dependent on the size and shape of the attached residue R, unlike the catemer motif, where the R group plays a critical role in determining whether it may exist.

We now consider how carboxylic hydrogen-bonded dimers interact, beginning with the possible ways coplanar carboxyl dimers juxtapose. The interdimer energy of such an arrangement was calculated as a function of the displacement of one of the dimers along the **L** and **M** directions (Figure 4).

Figure 4a presents the interdimer arrangement and Figure 4b presents the variation in energy as a function of displacement along **L**. A minimum was found for an interdimer separation at m = 5.75 Å. The van der Waals energy is relatively insensitive to displacement along **L** within the range examined. The Coulomb energy, and thus the total energy, favors almost equally two distinct arrangements, **6a** and **6b**. The most unstable state is shown in **6c**. There is strong structural evidence that arrangements similar to **6c**, with O(carbonyl)···O(hydroxyl) distances less than 3.5 Å, are avoided.[11] Indeed it is this repulsion that accounts for the

(16) I. Nahringbauer, *Acta Crystallogr., Sect. B*, **B34**, 315 (1978).
(17) I. Nahringbauer, *Acta Chem. Scand.*, **24**, 453 (1970).
(18) V. Benghiat and L. Leiserowitz, *J. Chem. Soc., Perkin Trans. 2*, 1763 (1972).
(19) C. T. Lin, I. C. Paul, and D. Y. Curtin, *J. Am. Chem. Soc.*, **96**, 3699 (1974).
(20) S. Abrahamsson, *Acta Crystallogr.*, **12**, 301 (1959).
(21) M. Fujinaga and M. N. G. James, *Acta Crystallogr., Sect. B*, **B36**, 3196 (1980).
(22) (a) T. Miyazawa and K. S. Pitzer, *J. Chem. Phys.*, **30**, 1076 (1959). (b) D. R. Lide, Jr., *Annu. Rev. Phys. Chem.*, **15**, 225 (1964).
(23) The OH···O bonds of the formic acid molecule, which was used as model, were linear and fixed at 2.65 Å, and each motif was planar.

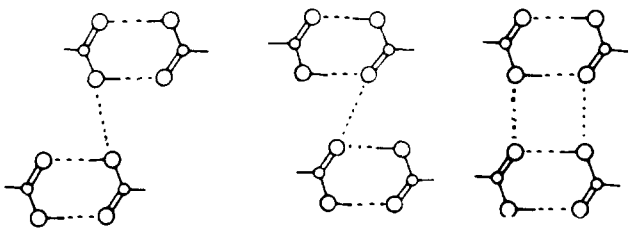

6a 6b 6c

fact that in the crystal structure of enantiomeric D-2-methyloctadecanoic acid,[20] which incorporates the rarely observed and least stable catemer motif **3c**, the plane of the carboxyl group is appreciably tilted with respect to the H-bonding 2_1 axis to increase the intermolecular distance between the neighboring O(carbonyl) and O(hydroxyl) atoms. Of the two energetically favorable motifs **6a** and **6b**, only the former has been observed in several crystal structures.[11] Almost all these crystal structures also contain intermolecular C–H···O(carbonyl) contacts, absent in our model calculations, which seem to further stabilize motif **6a**, as will be described in section 7.

6.2. Stacking of Carboxyl Dimers. The dimers of carboxylic acids RCO_2H form the distinctive stacking arrangements shown in **7** for a variety of R groups, suggesting that Coulomb forces play a primary role in determining the stacking arrangements.

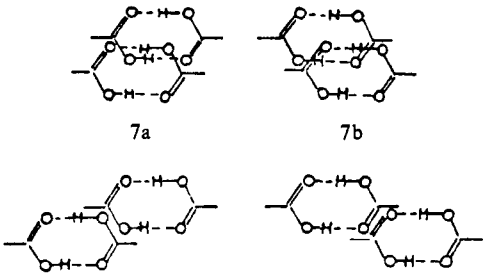

7a 7b

7c 7d

We have demonstrated[1] that the stacking geometries of primary amide dimers are determined primarily by Coulomb forces. In a similar way we calculated the energy of a stack of formic acid dimers as a function of offset (along directions **L** and **M**) between adjacent dimers, keeping the interplanar distance between dimers at 3.5 Å.[24]

The energy maps, presented in Figure 5, provide an insight into the preferred stacking arrangements of carboxyl dimers as well as into the phenomenon of order–disorder of carboxyl dimers, commonly observed in stacks.

The energy maps (Figure 5) exhibit approximate mirror symmetry about the **L** axis; hence, the energy of the stack remains almost the same upon interchanging the positions of the carbonyl oxygen and OH hydroxyl groups. Consequently, disorder of the carboxyl dimer, which will be analyzed in detail in section 6.3, is easily permitted in stacks, particularly for molecules that are symmetrically substituted with respect to the carbonyl and hydroxyl groups. The energy contour maps (Figure 5) also display the various interdimer arrangements, as observed in several carboxylic acid crystal structures: The circles a, b, c, and d encompass points that correspond to the four stacking motifs **7a–d** (i.e., to the relative offsets of the centers of the neighboring dimers in the stack). Arrangements **7a** and **7b**, denoted by points a and b, respectively, are almost equal in energy; similarly, arrangements **7c** and **7d**, denoted by points c and d, respectively, are about equally stable. The former arrangements, **7a** and **7b**, are more stable than **7c** and **7d** by 1.7 kcal/mol, due mainly to van der Waals energy (Figure 5b). This result is compatible with the relative frequency of arrangements **7a** and **7b** vs. **7c** and **7d**, as demonstrated in Table II, according to which 75% of the known crystal structures incorporate motifs **7a** and **7b**. The energy maps

(24) The average separation between H-bonded carboxyl dimers in a large variety of observed crystal structures is 3.5 Å.

Table II. The Four Modes (7a–d) of Interplanar Contact between Carboxyl Groups

compound	length of C–O bond, Å: in motif 7a,b	in motif 7c,d
α-tetrolic acid[18]	1.204	
β-tetrolic acid[18]		1.252
furane-α,α'-dicarboxylic acid[25]	1.205	
fumaramic acid[26]	1.209	
triclinic fumaric acid[27]		1.22
methyl fumarate[28]	1.276	
trans,trans-muconic acid,[29]		
molecule B	1.236	
molecule A	1.275	
methyl *trans,trans*-muconate[30]	1.23	
benzoic acid[31]		1.24
α-terephthalic acid[32]		1.28
β-terephthalic acid[32]	1.262	
p-chlorobenzoic acid[33]	1.253	
p-bromobenzoic acid[34]	1.225	
p-nitrobenzoic acid[35]		1.242
2-chlorobiphenyl-4-carboxylic acid[36]	1.205	
2'-chlorobiphenyl-4-carboxylic acid[37]	1.289	
2'-iodobiphenyl-4-carboxylic acid[38]	1.264	
o-fluorobenzoic acid[39]	1.255	
o-chlorobenzoic acid[40]	1.295	
o-bromobenzoic acid[41]	1.346	
1-naphthoic acid[42]	1.256	
2-naphthoic acid[a 43]		1.33

[a] The two C–O lengths of 1.33 and 1.37 in 2-naphthoic acid are obviously unreliable.

Table III. Calculated Differences in Crystal Energy (kcal/mol) of Trimesic Acid Containing Carboxyl Dimers of Groups I, II, and III and the Average Values of the $C–O_1$ ("Hydroxyl"), $C–O_2$ ("Carbonyl"), and O–H···O Distances (Å) of These Groups

group	ΔE	$\Delta(E+U)$	$\langle C–O_1 \rangle$	$\langle C–O_2 \rangle$	$\langle OH\cdots O \rangle$
I	1.6	1.5	1.319	1.218	2.65
II	0.3	0.5	1.277	1.244	2.64
III	0.0	0.0	1.255		2.64

were calculated by using formic acid dimers as models and so neglecting interactions involving residue groups. These interactions may account for the actual appearance of motifs **7c** and **7d**, as will be demonstrated in section 6.3 in an analysis on benzoic and terephthalic acids.

6.3. Order–Disorder (O/D) of the Carboxyl Dimer. We pursue the question of order–disorder (O/D) of the carboxyl dimer in terms of Coulomb and van der Waals energies in the distinctly different crystal structures of trimesic acid,[44] *trans,trans*-muconic acid,[29] and benzoic acid.[31] These three crystal structures were

(25) E. Martuscelli and C. Pedone, *Acta Crystallogr.*, **B24**, 175 (1968).
(26) V. Benghiat, H. W. Kaufman, L. Leiserowitz, and G. M. J. Schmidt, *J. Chem. Soc., Perkin Trans. 2*, 1758 (1972).
(27) A. L. Bednowitz and B. Post, *Acta Crystallogr.*, **21**, 566 (1966).
(28) L. Leiserowitz and C.-P. Tang, unpublished results.
(29) J. Bernstein and L. Leiserowitz, *Isr. J. Chem.*, **10**, 601 (1972).
(30) D. Rabinovitch and G. M. J. Schmidt, *J. Chem. Soc. B*, 286 (1967).
(31) (a) G. A. Sim, J. M. Robertson, and T. H. Goodwin, *Acta Crystallogr.*, **8**, 157 (1955). (b) J. Speakman, private communication.
(32) M. Bailey and C. J. Brown, *Acta Crystallogr.*, **22**, 387 (1967).
(33) R. S. Miller, I. C. Paul, and D. Y. Curtin, *J. Am. Chem. Soc.*, **96**, 6334 (1974).
(34) K. Ohkura, S. Kashino, and M. Haisa, *Bull. Chem. Soc. Jpn.*, **45**, 2651 (1972).
(35) S. S. Tavale and L. M. Pant, *Acta Crystallogr., Sect. B*, **B27**, 1479 (1971).
(36) H. H. Sutherland and T. G. Hoy, *Acta Crystallogr., Sect. B*, **B25**, 1013 (1969).

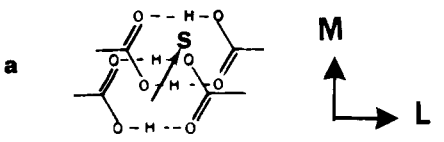

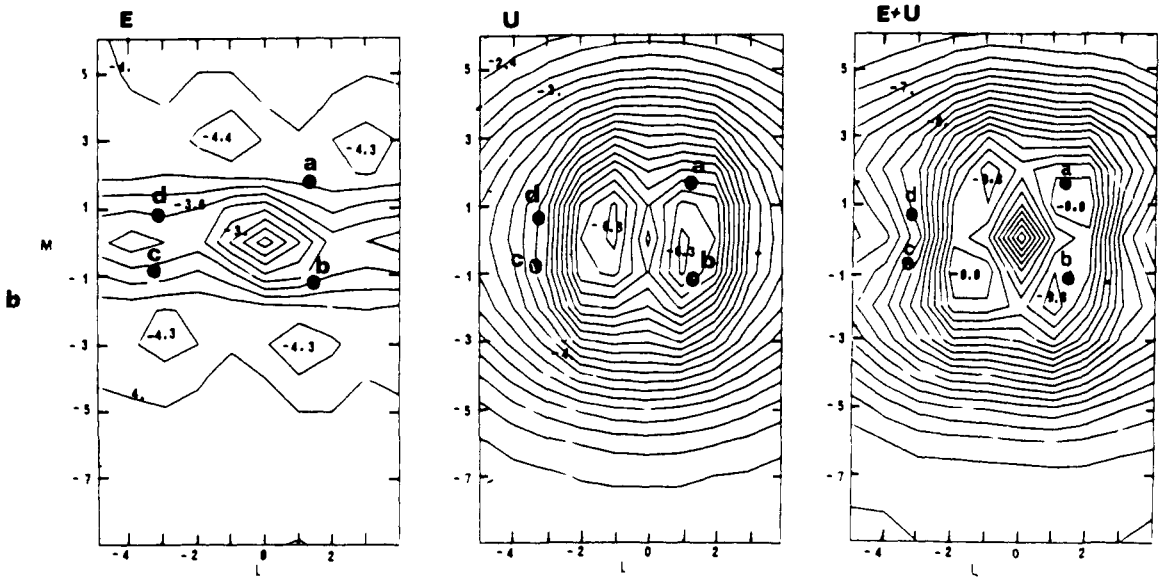

Figure 5. (a) Stacking arrangement of carboxyl acid dimers. (b) Variation in energy (kcal/mol) as a function of the *l,m* coordinates of the stack axis **S** = *l***L** + *m***M** + 3.5**N**. *E* = Coulomb energy; *U* = van der Waals energy. The various observed interdimer arrangements **7a–d** are marked **a–d**.

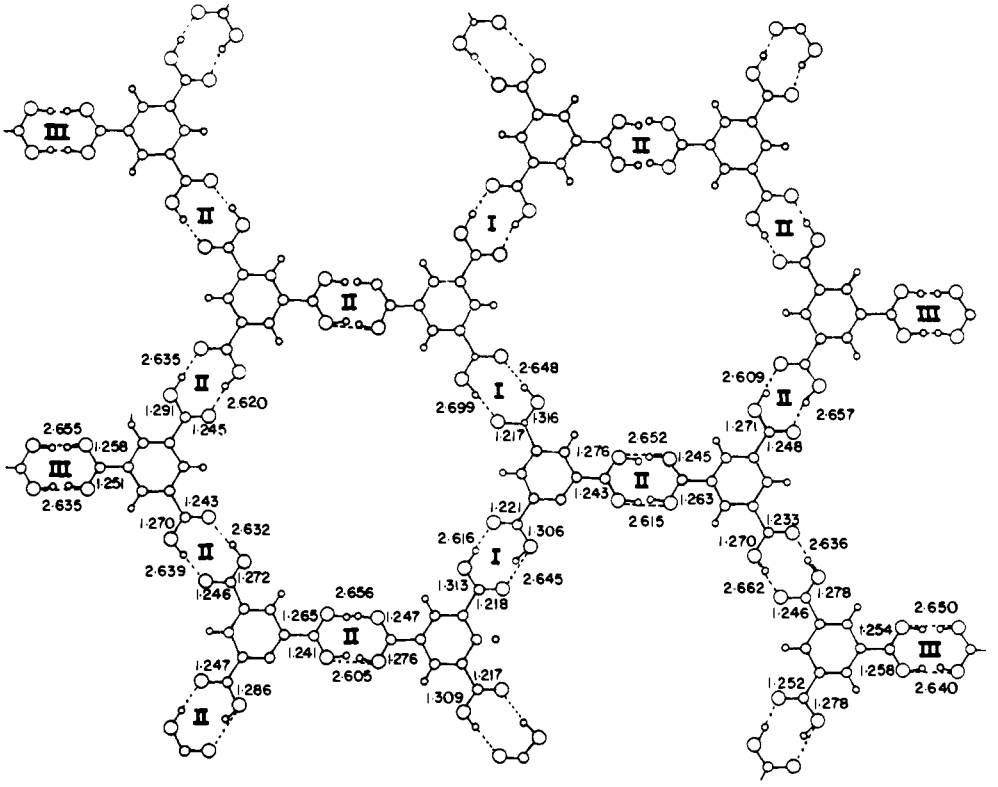

Figure 6. Trimesic acid structure. The space group is *C*2/*c* with six molecules per asymmetric unit forming the "chicken wire" motif. The different carboxyl groups belong to groups I, II, or III according to their order–disorder properties as specified by C–O bond lengths.

selected because each incorporates an internal check on the validity of the energy calculations. Entropy effects, which favor molecular disorder, were not included in this analysis.

The O/D properties of the carboxyl groups of trimesic acid may

(37) H. H. Sutherland, *Acta Crystallogr., Sect. B*, **B25**, 171 (1969).

(38) H. H. Sutherland, *Acta Crystallogr., Sect. B*, **B26**, 1217 (1970).

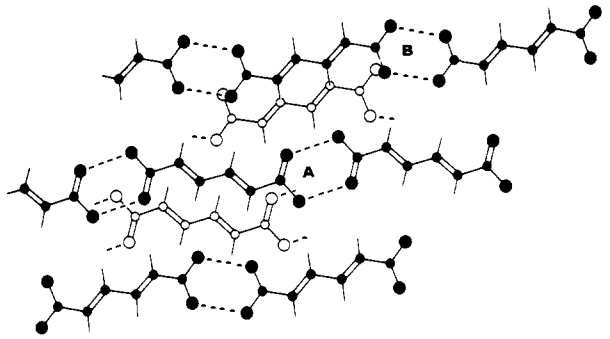

Figure 7. *trans,trans*-Muconic acid: intra- and interlayer arrangement. The two independent molecules A and B are labeled. The molecules with filled (or unfilled) atoms are almost coplanar.

be described in terms of their C–O bond lengths (Figure 6) and accordingly may be classified into three groups (Table III). Groups I, II, and III comprise carboxyl dimers that are ordered, partially ordered, and completely disordered, respectively.

We attempted to evaluate these observed O/D properties in terms of the difference in energy between the two conformers **8a** and **8b** as they appear in the crystal of trimesic acid.

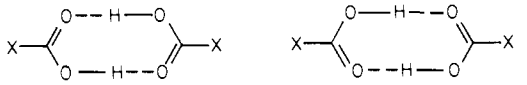

8a 8b

Ordered carboxyl groups, comprising normal carbonyl C=O and hydroxy C–OH bonds, were inserted into each of the crystallographically independent carboxyl sites for each of the two possible conformers **8a** and **8b**, and the lattice energy differences were determined. These energy differences were averaged for dimers belonging to the same category (I, II, or III), and the results are presented in Table III. For category I the crystal composed of the observed carboxyl conformer is more stable than that containing the alternative conformer by 1.5 kcal/mol, with the largest energy difference due to Coulomb forces. For category II this energy difference is 0.5 kcal/mol, in favor of the more prevalent conformer, with almost equal contributions from Coulomb and van der Waals forces. For category III the energy difference is zero by virtue of crystallographic symmetry. These calculations account for the observed degree of disorder in categories I, II, and III.

The crystal structure of *trans,trans*-muconic acid[29] provides a fine probe to analyze O/D in carboxyl dimers, since the structure contains two molecules per asymmetric unit in space group $P\bar{1}$, in which the dimer of one molecule (A) is ordered and the other (B) disordered (Figure 7).

The intralayer environments of molecules A and B are essentially identical so that the differences in O/D of their carboxyl groups must be due to their respective stacking arrangements along the 3.8 Å stack axis. We examined the O/D properties of molecules A and B by comparing the stacking energies of the synplanar (**9a**) and antiplanar (**9b**) conformers of molecules A and of B in their respective stacks.

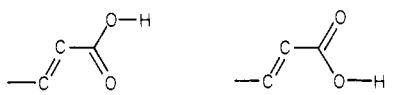

9a 9b

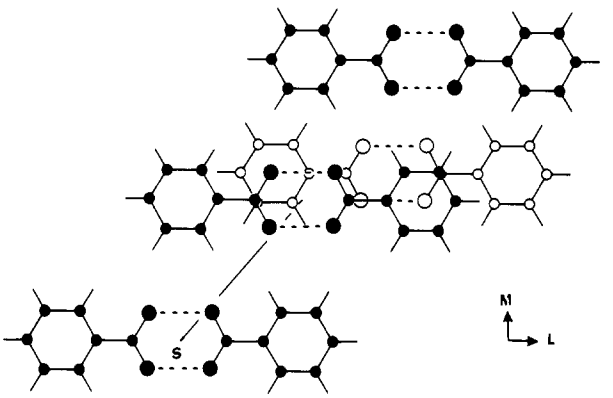

Figure 8. Benzoic acid structure. The molecules with filled atoms are almost coplanar and display the ribbon motif (**11**). The ribbon axis S = −4.824L − 5.745M + 0.52N.

For dimer A the difference in stacking energy of the (observed) syn and (postulated) anti conformers is 0.6 kcal/mol, in favor of the former. For dimer B, whose carboxyl group exhibits a mixture of the syn and anti conformers, the corresponding difference in stacking energy is 0.2 kcal/mol, in favor of the antiplanar conformer. There is a great deal of experimental evidence in crystal structures of α,β-unsaturated carboxylic acids $RHC{=}CHCO_2H$ that of the two possible conformers the synplanar is the more stable.[11] Moreover, according to ab initio calculations,[8] the intramolecular energy difference, in favor of the synplanar conformer, is 0.5 kcal/mol. Thus both intra- and intermolecular forces appear to act in concert for molecule A, so stabilizing the synplanar conformer, whereas these forces act in opposite directions for molecule B, thus inducing disorder.

Benzoic acid exhibits disorder at room temperatures.[31] According to a neutron diffraction analysis, the crystal structure at 5 K is probably free of disorder and consists of dimers in the A configuration[31b] (**10a**) (or **7a**) as opposed to the B configuration (**10b**) (or **7b**).

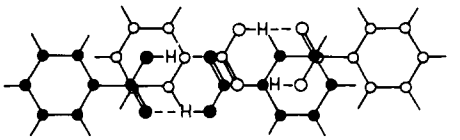

10a

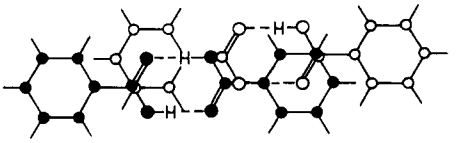

10b

Atom–atom potential energy calculations by Unemura and Hayashi[45] employing partial atomic charges derived by CNDO calculations indicated that an ordered crystal, composed of A molecules (**10a**), is more stable than a crystal composed of B molecules (**10b**) by 0.2–0.4 kcal/mol. We have found a similar result; a crystal composed of benzoic acid molecules in the A configuration is more stable than that composed of molecules in the B configuration by 0.28 kcal/mol, totally due to Coulomb energy. At room temperature this energy difference is $\simeq {}^1/_2KT$, so accounting for the disorder. These calculations indicate that it is possible to account for the presence of order–disorder in energy terms. The entropy term, maximally $RT \ln 2$ (~0.4 kcal/mol at room temperature), tends to induce disorder when the entropy contribution is comparable to the energy difference between the two ordered states **8a** and **8b**.

6.4. Ribbon Arrangement in Substituted Benzoic Acids. The ribbon motif (**11**) displayed by benzoic acid (Figure 8) is a common feature of several substituted benzoic acids.[11] This motif demonstrates the ease for such molecules to display carboxyl disorder, for it is clear that the O(carbonyl) and O(hydroxyl)

(39) J. Krausse and H. Dunken, *Acta Crystallogr.*, **20**, 67 (1966).
(40) G. Ferguson and G. A. Sim, *Acta Crystallogr.*, **14**, 1262 (1961).
(41) G. Ferguson and G. A. Sim, *Acta Crystallogr.*, **15**, 346 (1962).
(42) J. Trotter, *Acta Crystallogr.*, **13**, 732 (1960).
(43) J. Trotter, *Acta Crystallogr.*, **14**, 101 (1961).
(44) D. J. Duchamp and R. E. Marsh, *Acta Crystallogr., Sect. B*, **B25**, 5 (1969).
(45) J. Unemura and S. Hayashi, *Bull. Chem. Inst. Kyoto Univ.*, **53**, 180 (1975).

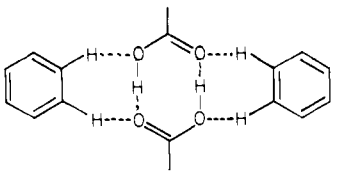

11

groups have similar environments within the ribbon motif. Thus the presence of disorder in benzoic acid, discussed above, may be atrributed almost wholly to stacking forces along the *b* axis. The tendency to form the ribbon motif may be understood in terms of the change in energy as a function of the variation in offset between two coplanar benzoic acid dimers, as shown in Figure 9. From Figure 9 it is clear that van der Waals forces play the primary role in determining the offset between the adjacent dimers. The variation in Coulomb energy is much flatter and accounts only for approximately 10% of the total interaction energy between the dimers. Nevertheless, the position of the minimum in Coulomb energy is very close to that of the minimum of total energy, whose position almost coincides with the observed arrangement (see Figure 9).

Terephthalic acid[32] is dimorphic. Both forms (α and β) have similar layer structures (Figures 10 and 12) incorporating the ribbon motif (**11**). In a manner akin to the calculations done on benzoic acid, the layer energy of terephthalic acid was calculated as a function of the offset between the coplanar hydrogen-bonded chains forming the layer (Figure 11). The van der Waals energy curve exhibits a double minimum, with a hump of 0.5 kcal/mol. The minimum in Coulomb energy falls at a point close to the van der Waals energy minimum. The layer structure that corresponds to the calculated energy minimum is very close to that of the observed structure (see Figures 10 and 11).

The essential difference between the α and β forms of terephthalic acid lies in their different interlayer arrangements (cf. Figures 10 and 12) yielding carboxyl stacking (**7a,b** vs. **7c,d**).

Both crystal structures are triclinic $P\bar{1}$ with one molecule per unit cell, and the difference between the α and β forms lies in the degree of offset between adjacent layers. The calculated crystal energy as a function of offset between adjacent terephthalic acid layers exhibits two minima whose positions correspond very closely to the observed interlayer offsets (Figure 13).

7. C–H···O(Carbonyl) Interaction in Carboxylic Acids

Studies of various packing arrangements in carboxylic acids have indicated that strong attractive C–H···O interactions play a decisive role in stabilizing certain packing arrangements and in fixing molecular conformation.[11] Here we will try to put these deductions on a sound footing via energy calculations on serveral observed motifs incorporating the C–H···O contact.

We first consider the dimer **12**, found in several structures,

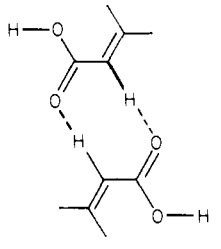

12

including the α and β forms of fumaric acid,[27,46] α-*trans*-cinnamic acid,[47] *p*-chloro-*trans*-cinnamic acid,[48] methyl fumarate,[28,49] and methyl *trans,trans*-muconate.[30]

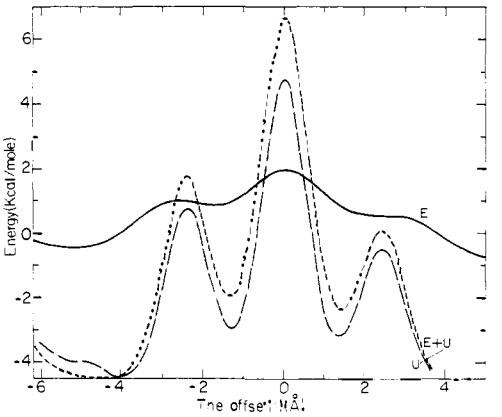

Figure 9. Benzoic acid: the variation in energy of the ribbon motif (**11**) as a function of the offset in **L** between the almost coplanar benzoic acid dimers (see Figure 8). The separation between dimers along **M** and **N** was kept at the observed distances (−5.75, 0.52 Å, respectively). The energy minimum occurs at $l = -4.5$ Å, compared with the observed values of $l = -4.8$ Å.

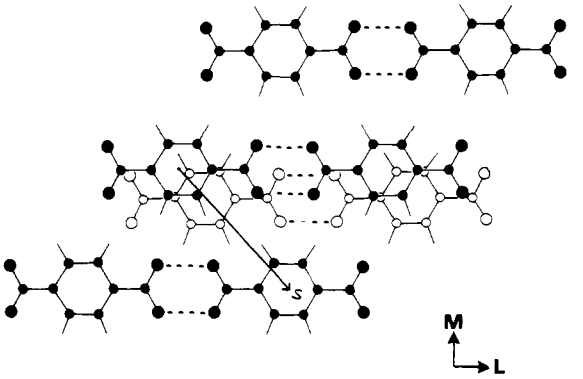

Figure 10. Terephthalic acid: inter- and intralayer structures incorporating the ribbon motif (**11**). The ribbon axis **S** = 4.89**L** − 5.81**M** + 0.41**N**. The interlayer axis **S′** = −1.09**L** + 1.47**M** − 3.27**N**. The molecules with filled atoms are almost coplanar and display the ribbon motif (**11**).

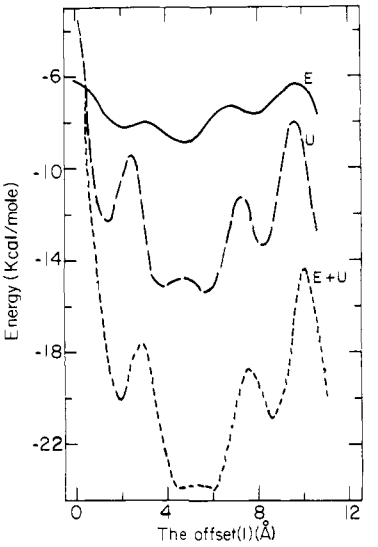

Figure 11. Variation in the layer energy of terephthalic acid as a function of offset along **L** between coplanar H-bonded chains of terephthalic dimers (see filled atoms in Figure 10). The separation between the chains along **M** and **N** was kept fixed at the observed distances. The minimum in energy occurs at $l = 4.5$ Å, compared with the observed value of 4.9 Å (see Figure 10).

As a model molecule we chose allenecarboxylic acid.[50] We determined the energy of this coplanar and centrosymmetric dimer

(46) C. J. Brown, *Acta Crystallogr.*, **21**, 1 (1966).
(47) J. Ladell, T. R. R. McDonald, and G. M. J. Schmidt, *Acta Crystallogr.*, **9**, 195 (1956).
(48) J. P. Glusker, D. E. Zacharias, and H. L. Carrell, *J. Chem. Soc., Perkin Trans. 2*, 68 (1975).
(49) C.-P. Tang, M.Sc. Thesis, The Feinberg Graduate School, The Weizmann Institute of Science, Rehovot, Israel, 1974.

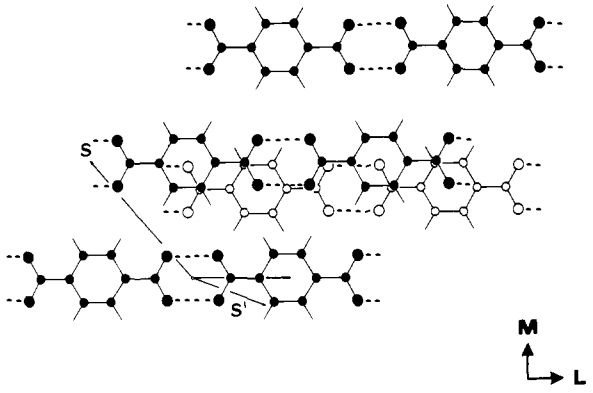

Figure 12. β-Terephthalic acid: Intra- and interlayer structures. Interlayer vector S' = 3.67L + 0.60M-3.38N. The molecules with filled atoms are almost coplanar and display the ribbon motif (**11**).

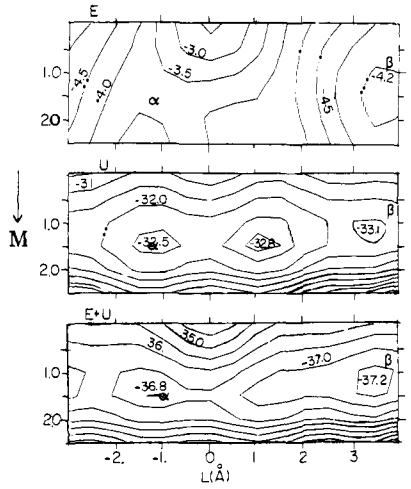

Figure 13. Terephthalic acid: the variation in crystal energy (kcal/mol) as a function of the offset between layers. The observed offset values of the α and β forms are marked α and β on the energy diagrams.

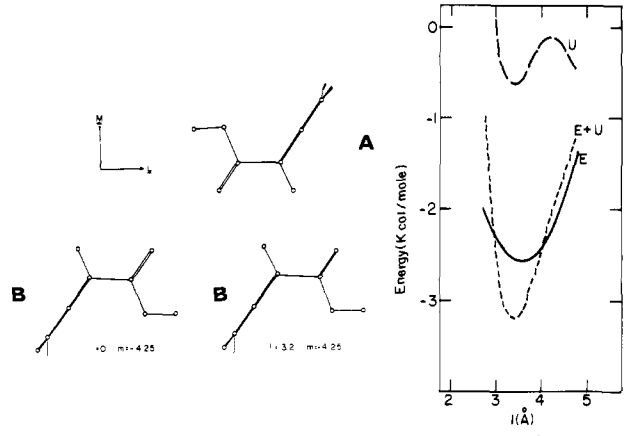

Figure 14. Variation in energy as a function of the offset along **L** between two coplanar centrosymmetrically related molecules of allenecarboxylic acid at a distance $m = -4.25$ Å. Molecule **B** was moved relative to molecule A. Two positions of **B** are shown: the starting position ($l = 0$) and that corresponding to the minimum energy ($l = 3.2$ Å). E = Coulomb energy; U = van der Waals energy.

as a function of offset along directions **L** and **M**. The variation in energy as a function of relative movement along **L** at a distance $m = -4.25$ Å, which corresponds to the energy minimum, is shown in Figure 14. A distinct minimum is found for the Coulomb energy corresponding to a linear C—H···O contact. The variation

(50) Accurate electrostatic properties for this molecule were available from the low-temperature X-ray diffraction study of allenedicarboxylic acid-acetamide.[8]

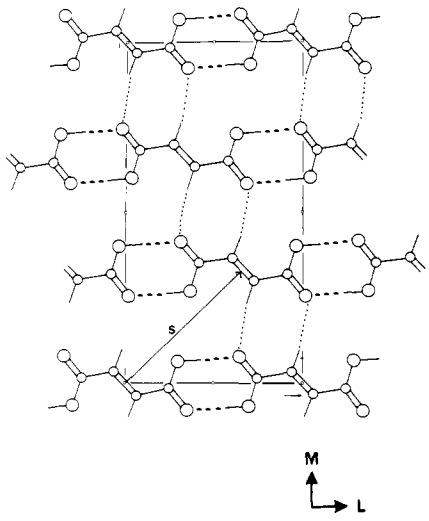

Figure 15. Fumaric acid layer structure. The layer axis **S** = 5.02L + 5.07M − 0.16N (components in Å).

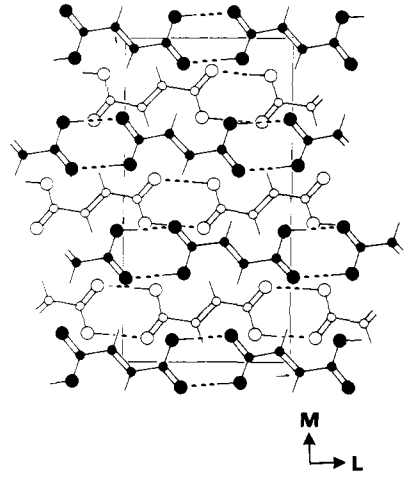

Figure 16. β-Fumaric acid: monoclinic form. Two neighboring layers (open and filled atoms, respectively) related by 2_1 symmetry are shown.

in van der Waals energy is much shallower but with a minimum at almost the same position as found for the Coulomb term. The calculated energy of the dimer at the minimum is −3.2 kcal/mol, of which 80% is Coulomb energy. Thus there is little doubt that Coulomb forces play the dominant role in determining the directional properties of the C—H···O interaction.

It is noteworthy here that the energy of the observed acetic acid dimer (**13**), which incorporates an O–H···O bond and a C–H···O

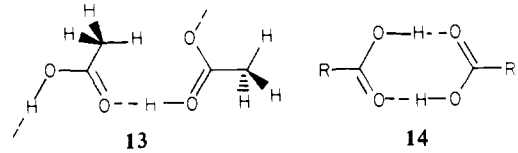

13 **14**

contact, is −4.25 kcal/mol, almost 70% due to Coulomb forces. The energy of acetic acid in the normal dimer form (**13**) is −6.5 kcal/mol. If we ascribe half this amount to each O–H···O bond, it appears that the C–H···O interaction contributes 1.0 kcal/mol to the stabilization of the observed dimer (**13**).

We next consider fumaric acid, which incorporated C–H···O contacts in its layer structure. For the purpose of analysis it has the advantage of being dimorphic[27,46] ($P\bar{1}$, $Z = 1$; $P2_1/c$, $Z = 6$); both modifications exhibit the antiplanar C=C—C=O conformation and similar layer structures[27,46] (Figure 15).

In the monoclinic form[46] the layers are related by 2_1 axes (Figure 16); in the triclinic form[27] the layers are related by translation (Figure 17).

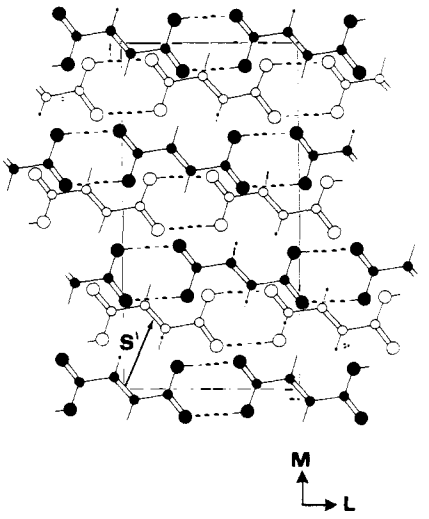

Figure 17. Fumaric acid: interlayer structure of the triclinic form. Interlayer vector S' = 1.30L + 3.08M + 2.99N. Molecules with filled (or empty) atoms are almost coplanar.

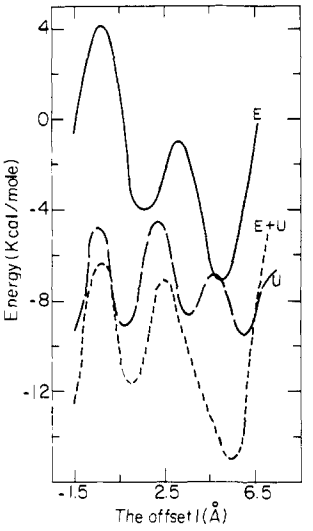

Figure 18. Variation in layer energy (E = Coulomb energy; U = van der Waals energy) for the observed antiplanar (**9b**) conformer of fumaric acid as a function of the offset along **L** between H-bonded chains, keeping the interchain separation along **M** fixed at the observed value of 5.07 Å. The minimum is at l = 5.0 Å, which is identical with the observed value (see Figure 15).

It has already been argued[11] that since intramolecular forces favor the synplanar C=C—C=O conformer (**9a**) the antiplanar C=C—C=O conformation (**9b**) of fumaric acid must be induced primarily by intralayer forces, interlayer interactions being a less likely explanation, since the packing of the layers is different in the two crystal structures. To verify these arguments on a quantitative level, we carried out the following calculations: the energy of the layer was determined as a function of the offset between adjacent hydrogen-bonded chains within the layer for both (observed) anti- and (hypothetical) synplanar conformers. The resulting Coulomb energy curve for the antiplanar conformer (Figure 18) displays a distinct minimum of −7 kcal/mol for an offset corresponding to the observed layer structure. The van der Waals energy curve yields several minima in the range −8 to −9 kcal/mol, suggesting several possible arrangements. The combined energy surface (E + U in Figure 18) yields two distinct minima of −12 and −15 kcal/mol, the latter with an offset corresponding to the observed structures. Thus it appears that the C–H···O(carbonyl) interaction plays an important role in stabilizing the observed layer structure.

Indeed all the α,β-unsaturated acids R—C(α)H=C(β)H—CO_2H that incorporate the antiplanar C=C—C=O conformer,

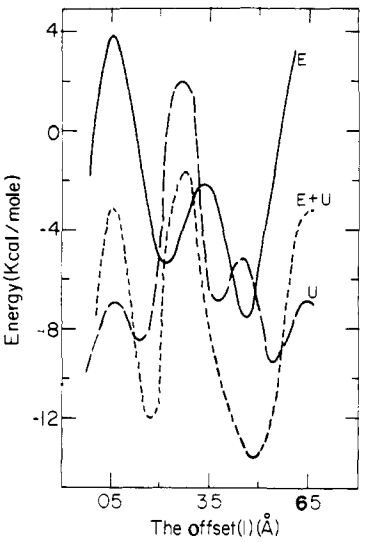

Figure 19. Variation in layer energy (E = Coulomb energy; U = van der Waals energy) for the synplanar conformer (**9a**) of fumaric acid as a function of the offset along **L** between H-bonded chains, keeping the interchain separation along **M** fixed at the observed value of 5.07 Å. The energy minimum occurs at l = 5.2 Å, which corresponds to the observed value of the antiplanar conformer (**9b**) (see Figure 15).

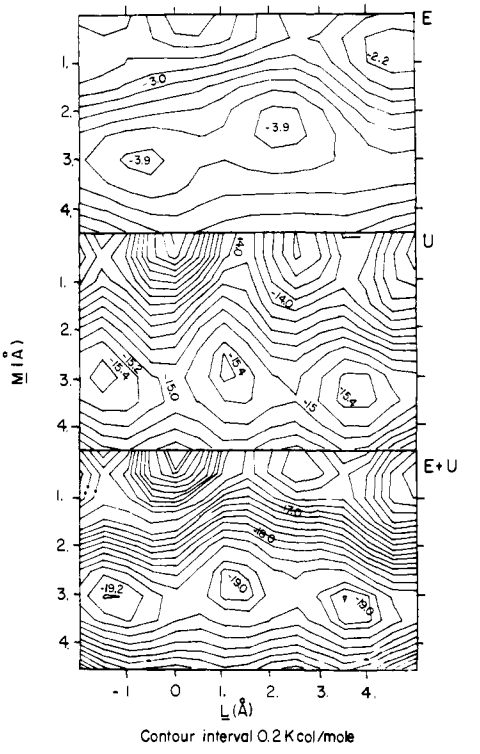

Figure 20. Triclinic fumaric acid: variation in crystal energy (kcal/mol) (E = Coulomb energy; U = van der Waals energy) as a function of offset between layers. The observed value for the triclinig form is l = 1.3, m = 3.0 Å (see Figure 17).

i.e., fumaric acid,[27,46] α-*trans*-cinnamic acid,[47] *p*-chloro-*trans*-cinnamic acid,[48] methyl *trans,trans*-muconate,[30] and methyl fumarate,[11,49] form this C–H···O contact.

The variation in layer energy of fumaric acid as a function of the offset between adjacent H-bonded chains for the hypothetical synplanar conformer is shown in Figure 19. The minimum energy is −13.8 kcal/mol, corresponding to a layer structure in which a C–H···O(hydroxyl) contact replaces the observed C–H···O(carbonyl) contact. This hypothetical fumaric acid struture, incorporating the synplanar conformation, is 1.1 (14.9 − 13.8) kcal/mol less stable than the observed layer that incorporates the antiplanar conformer. According to MO calculations,[8] the antiplanar con-

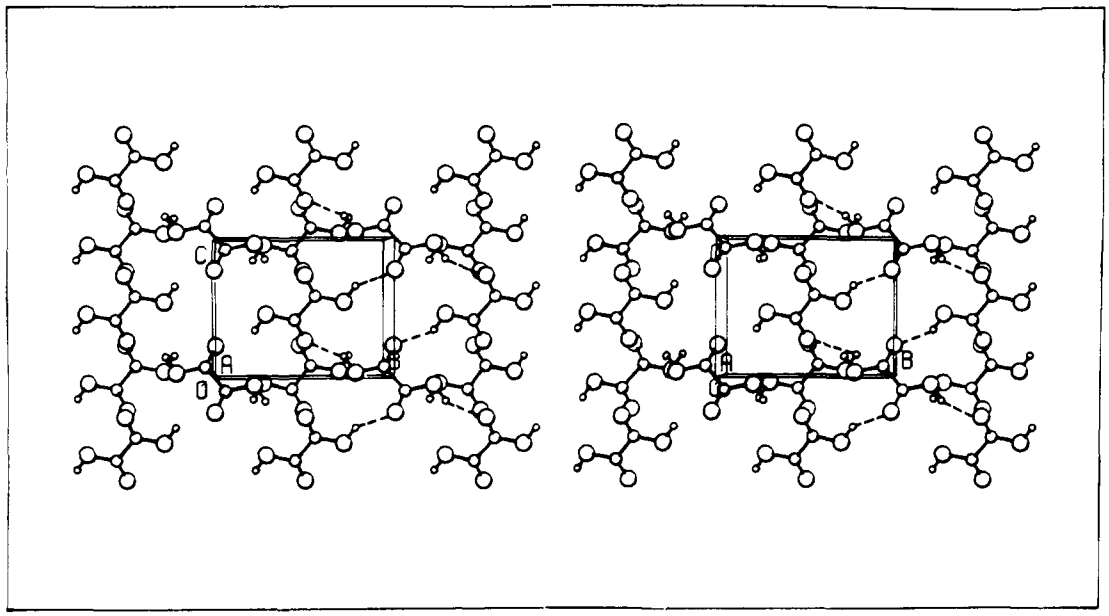

Figure 21. Stereoscopic view of α-oxalic acid seen along a.

former is 0.5 kcal/mol less stable than the synplanar one. Thus the intermolecular stabilization energy of 1.1 kcal/mol is just sufficient to compensate for the calculated loss of 1.0 kcal/mol (0.5 kcal/mol for each of the carboxylic groups) in adopting the antiplanar conformation. Although these results are in the right direction, it appears to us that the calculated stabilization energy of 1.1–1.0 kcal/mol is too low.

We next calculated the crystal energy of the triclinic form of fumaric acid as a function of offset of adjacent layers of the observed structure (Figure 20). The observed structure lies in a region of minimum energy. The calculated lattice energies of the observed triclinic and monoclinic forms are −24.2 and −25.4 kcal/mol, respectively, in agreement with the greater stability of the monoclinic crystal form.

All these energy calculations provide additional and forceful evidence of the attractive and specific nature of the C–H···O(carbonyl) interaction, which has long been a matter of debate.

8. Generation of Possible Crystal Structures

The reason a given molecule appears in its particular crystal structure may, for many systems, be more easily understood by constructing an ensemble of possible packing arrangements and eliminating the least stable arrangements therefrom. This procedure was adopted by (a) Derissen and Smit[2] to pinpoint why acetic acid forms the catemer motif in the solid, as opposed to the commonly observed cyclic dimer, but with inconclusive results, and by (b) Hagler and Leiserowitz[5] to establish why adipamide adopts a rare (and less favorable) hydrogen-bonding structure.

In this section we shall examine the role played by Coulomb and van der Waals forces in determining the overall crystal structure for the α and β forms of oxalic acid and for formic acid by inserting given hydrogen-bonding arrangements into various crystal structures.

8.1. α Form of Oxalic Acid. α-Oxalic acid[51] crystallizes in space group *Pbca*. The molecules are interlinked by O—H···O bonds in the catemer motif, generating a *bc* hydrogen-bonded layer (Figure 21). The symmetry of this layer may be defined as $P(1)2_1/c1$. This nomenclature fixes the symmetry elements along the axes b and c but not along a; the symbol (1) specifies that along a the symmetry is not fixed. By assigning the possible symmetry elements with respect to a, we generate various possible space groups in which the layer may be incorporated. The possible space groups are $P2_1/n2_1/c2/a$ (i.e., *Pnca*), $P2_1/c2_1/c2_1/n$ (i.e., *Pccn*), $P2_1/m2_1/c2_1/n$ (i.e., *Pmcn*), $P12_1/c1$ (i.e., $P2_1/c$), and $C12_1/c1$ (i.e., $C2/c$). We generated various crystal structures by incorporating the hydrogen-bonded layer of α-oxalic acid in these space groups. For the orthorhombic space groups *Pnca*, *Pccn*, and *Pmcn* the only variable is the length of the a axis (given the hydrogen-bonding geometry as by and large fixed). For the monoclinic space groups $P2_1/c$ and $C2/c$ there are two degrees of freedom: the length of the a axis and the β angle. We calculated the Coulomb and van der Waals contributions to the lattice energies of all these various crystal structures, and the results are summarized in Table IV. All these arrangements, but for the $P2_1/c$ structure, were found to be significantly less stable than the observed structure.

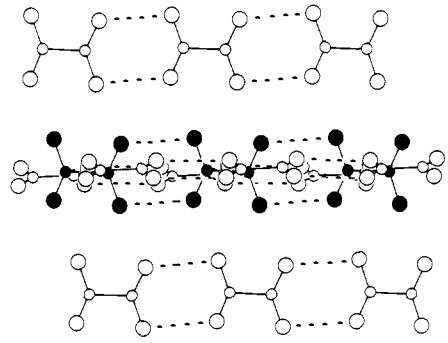

Figure 22. β Form of oxalic acid displaying the "T" structure (if viewed along the H-bonding chain), in which planes of the c-glide-related H-bonded chains are perpendicular to each other. The axes of these chains are parallel to a.

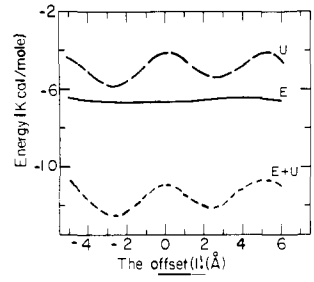

Figure 23. Variation in energy of the glide-related molecules of β-oxalic acid as a function of the offset along the a axis between the c-glide-related chains forming the "T" structure (see Figure 22). The observed structure corresponds to an offset of l = 2.4 Å.

8.2. β Form of Oxalic Acid. The β form of oxalic acid[51] appears in space group $P2_1/c$, with hydrogen-bonded chains parallel to

(51) J. C. Derissen and P. H. Smit, *Acta Crystallogr., Sect. B*, **B30**, 2240 (1974).

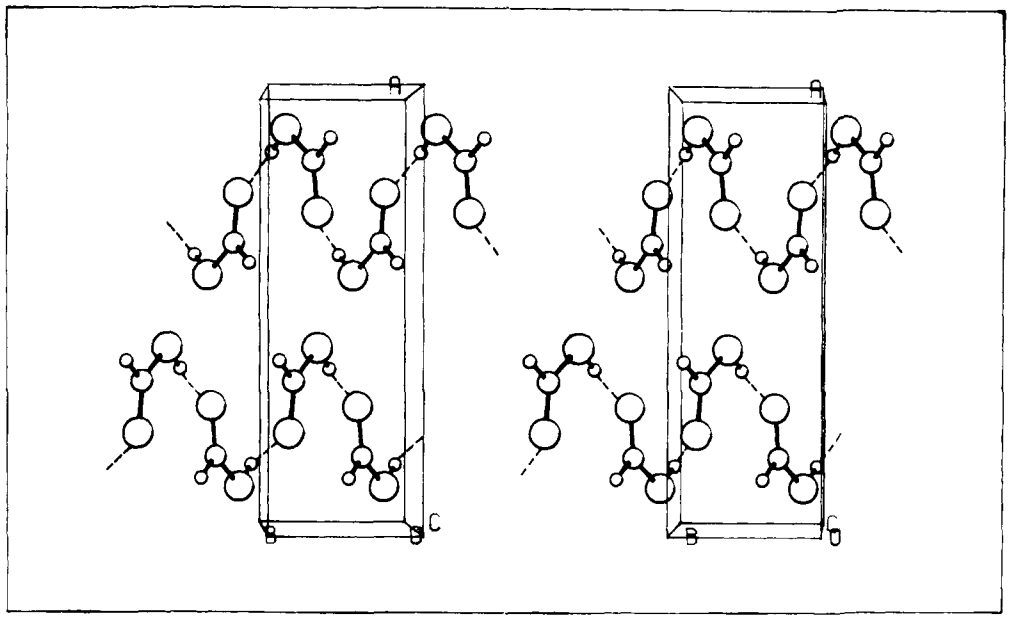

Figure 24. Formic acid: catemer motif.

Table IV. α-Oxalic Acid; the Crystal Energy (kcal/mol) of Various Hypothetical Crystal Structures

cryst structure	E	$E + U$
Pbca[a]	−8.00	−19.82
Pnca	−6.44	−14.03
Pccn	−2.57	>0
Pmcn	−0.26	>0
$P2_1/c$	−0.75	−16.50

[a] Observed structure.

the *a* axis. The nearest-neighbor chains, related by the *c* glide, as viewed along the *a* axis form a "T"-shape structure (Figure 22). We investigated the relative roles played by the Coulomb and van der Waals forces in fixing the offset between these glide-related chains, this offset being determined by the angle β between the *a* and *c* axes. According to Figure 23, which displays the variation in energy as a function of the offset between the glide-related chains, the Coulomb energy of interaction between two glide-related chains is almost constant. On the other hand, there is a pronounced variation in van der Waals energy in a range of 2.0 kcal/mol. Therefore the offset between the chains is determined primarily by the van der Waals forces, despite the polar nature of the carboxyl groups.

The question arises whether it is possible to arrange the hydrogen-bonded chains of β-oxalic acid in alternative motifs that will yield hypothetical structures as stable (or more so) as the observed one. To check this point, we have generated an ensemble of possible packing arrangements. We first note that in all these structures the chain axes are parallel, because it was deduced,[52] on packing considerations, that for centrosymmetric hydrogen-bonded chains, with a translation repeat appreciably less than 6.8 Å, the crystal structure will adopt an arrangement in which all the chain axes are parallel. Furthermore, we may discard orthorhombic space groups incorporating the "T" structure on energy considerations, since the offset between the glide-related chains in the observed structure, corresponding to a β angle of 115.5°, is far different from 90°, as would be required in an orthorhombic packing. An angle of 90° (corresponding to $l = 0$ in Figure 23) would incur an energy loss of 1.5 kcal/mol. Finally, the monoclinic space groups containing a dyad axis, such as $P2/c$, may be excluded since in these space groups parallel chains containing polar groups would have to be related by twofold symmetry, inducing unfavorable repulsive interactions between like polar atoms. Thus

(52) L. Leiserowitz and A. T. Hagler, *Proc. R. Soc. London, Ser. A.*, in press.

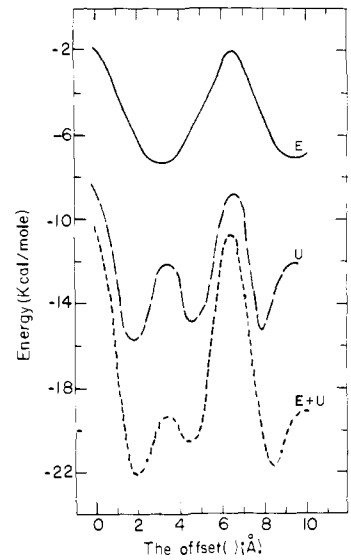

Figure 25. Variation in energy as a function of offset (l) between neighboring catemer chains of formic acid related by the short axis *b*. The offset between neighboring catemer chains in the observed structure is l = 1.96 Å, and the offset corresponding to the energy minimum is l = 2.0 Å.

we consider space group $P\bar{1}$, in which all chains are parallel. We attempted to arrange the H-bonded chains in all possible ways. In all cases, the calculated energy minima were distinctly higher, by at least 3 kcal/mol, than the calculated energy of the observed structure.

8.3. Formic Acid. Formic acid[16] crystallizes in space group $Pna2_1$, with a = 10.24, b = 3.54, and c = 5.36 Å. The molecules appear in the catemer motif (Figure 24), interlinked by O–H···O bonds along the $b + c$ axis via an *n* glide. These catemer chains form close-packed (100) layers, which make contact with each other via an *a* glide. Acetic acid[17] is almost isostructural with formic acid, implying that their overall packing has distinct advantages over alternative arrangements.

We have attempted to ascertain whether there are any other reasonable alternative modes of combining the hydrogen-bonded chains to form viable crystals. We first determined the variation in energy as a function of offset between neighboring catemer chains separated by an interplanar distance of 3 Å along the *b* axis of 3.5 Å (Figure 25). Here we note that space group $Pna2_1$ imposes a restriction of 90° on the angle α between the *b* and *c*

axes and thus on the offset between the nearest-neighbor chains along *b*. The energy curves (Figure 25) display minima both in Coulomb and in van der Waals terms for an offset similar to the observed arrangement. Thus the calculated degree of offset in the *bc* plane is completely compatible with that of the observed orthorhombic structure. We next examined ways of juxtaposing the (100) layers via symmetry elements, other than the observed, to yield different crystal structures. Space group $Pn11$ was obtained by relating the (100) layers by translation along the *a* axis. Space group $P2_1/n11$ was generated via a 2_1 axis relating the (100) layers. Space group $P112_1$ was generated by replacing the *n* glide, forming the catemer chain, by a 2_1 axis.[53] This change is possible because the catemer chain is almost coplanar, and thus the *n* glide and the 2_1 axis yield almost the same contacts. All three alternative crystal structures were found to be appreciably less stable (by at least 5 kcal/mol) than the observed structure.

In summary, we have demonstrated for the two forms of oxalic acid and for formic acid that the observed crystal structure is more stable than an assortment of possible alternative packing arrangements, each incorporating the hydrogen-bonding motif of the observed structure.

(53) It is noteworthy that tetrolic acid,[18] which appears in the catemer motif, crystallizes in space group $P2_1$.

9. Summary

Information contained in experimental electron density distributions was used to improve the electrostatic parameters of the carboxyl group and thus to obtain a better estimate of the Coulomb intermolecular energies in crystals of carboxylic acids.

By energy calculations using the improved parameters, we were able to account for various characteristic properties of molecular packing of carboxylic acids.

Acknowledgment. We thank Professor F. Hirshfeld for his advice and a critical reading of the manuscript. This research was supported by a grant from the United States–Israel Binational Science Foundation (BSF), Jerusalem, Israel.

Registry No. Fumaric acid, 110-17-8; oxalic acid, 144-62-7; formic acid, 64-18-6; terephthalic acid, 100-21-0; benzoic acid, 65-85-0; trimesic acid, 554-95-0; (*E,E*)-muconic acid, 3588-17-8; formamide, 75-12-7; tetrolic acid, 590-93-2; furan-α,α'-dicarboxylic acid, 3238-40-2; fumaramic acid, 2987-87-3; methyl fumarate, 2756-87-8; methyl (*E,E*)-muconate, 10085-20-8; *p*-chlorobenzoic acid, 74-11-3; *p*-bromobenzoic acid, 586-76-5; *p*-nitrobenzoic acid, 62-23-7; 2-chlorobiphenyl-4-carboxylic acid, 5728-41-6; 2′-chlorobisphenyl-4-carboxylic acid, 3808-93-3; 2′-iodobiphenyl-4-carboxylic acid, 3808-95-5; *o*-fluorobenzoic acid, 445-29-4; *o*-chlorobenzoic acid, 118-91-2; *o*-bromobenzoic acid, 88-65-3; 1-naphthoic acid, 86-55-5; 2-naphthoic acid, 93-09-4.

Electronic Structures of Bent-Sandwich Compounds of the Main-Group Elements: A Molecular Orbital and UV Photoelectron Spectroscopic Study of Bis(cyclopentadienyl)tin and Related Compounds

S. G. Baxter,[1a] A. H. Cowley,*[1a] J. G. Lasch,[1a] M. Lattman,*[1b] W. P. Sharum,[1b] and C. A. Stewart[1a]

Contribution from the Departments of Chemistry, The University of Texas at Austin, Austin, Texas 78712, and Southern Methodist University, Dallas, Texas 75275. *Received July 27, 1981*

Abstract: An SCF Xα scattered-wave (Xα-SW) calculation has been performed on the bent-sandwich molecule $(\eta^5\text{-}C_5H_5)_2Sn$ (stannocene). The Xα-SW calculation revealed that the highest occupied MO's ($6a_2$ and $9b_2$) are π type and highly localized on the cyclopentadienyl rings. In order of decreasing energy, the MO's associated with the bonding of the C_5H_5 group to Sn are $11a_1$, $6b_1$, $10a_1$, $8b_2$, and $9a_1$. Of these MO's, the one exhibiting the largest tin lone pair character is $10a_1$. The MO's $5a_2$, $5b_1$, and $8a_1$ to $2b_2$ inclusive are σ_{CC} and σ_{CH} in character, highly localized on the C_5H_5 rings, and comparable in energy to the corresponding MO's of ferrocene. An MNDO calculation on $(C_5H_5)_2Si$ and the isoelectronic species $[(C_5H_5)_2P]^+$ indicated that a bis(pentahapto) structure is the global minimum in both cases. The sequences of the higher MO's of $(\eta^5\text{-}C_5H_5)_2Si$ and $(\eta^5\text{-}C_5H_5)_2Sn$ as computed by the MNDO and Xα-SW methods, respectively, are in good mutual agreement. He(I) ultraviolet spectra (UV PES) have been measured for $(\eta^5\text{-}C_5H_5)_2Sn$, $(\eta^5\text{-}C_5H_5)_2Pb$, $(\eta^5\text{-}Me_5C_5)_2Sn$, and $(\eta^5\text{-}Me_5C_5)_2Pb$. The UV PES data have been interpreted with the aid of theoretical ionization energies computed for $(\eta^5\text{-}C_5H_5)_2Sn$ by the transition-state method. The synthesis of $(\eta^5\text{-}Me_5C_5)_2Pb$ is described.

The electronic structures and patterns of stability of the π complexes of the transition and f-block elements are now understood reasonably well. By contrast, much less is known about compounds that feature multihapto bonding between the main-group elements and carbocyclic ligands. Some progress has been made toward understanding π-bonded cyclopentadienyl compounds of the group 1A and 2A elements such as $(\eta^5\text{-}C_5H_5)Li$[2] and $(\eta^5\text{-}C_5H_5)BeX$[3] and the intriguing molecule beryllocene, $(C_5H_5)_2Be$.[4] However, our understanding of the bent-sandwich molecules of the group 4A elements is much less complete and, in fact, molecular orbital (MO) calculations on such systems are confined to one semiempirical MO study of stannocene, $(\eta^5\text{-}C_5H_5)_2Sn$.[5] The present paper represents an attempt to develop a theoretical model for bent-sandwich molecules. We were particularly interested in the nature of the bonding between the

(1) (a) University of Texas at Austin. (b) Southern Methodist University.
(2) (a) Janoschek, R.; Diercksen, G.; Preuss, H. *Int. J. Quantum Chem. Symp.* **1967**, *1*, 205–208. (b) Alexandratos, S.; Streitwieser, A., Jr.; Schaefer, H. F., III *J. Am. Chem. Soc.* **1976**, *98*, 7959–7962.
(3) (a) Dewar, M. J. S.; Rzepa, H. S. *J. Am. Chem. Soc.* **1978**, *100*, 777–784. (b) Jemmis, E. D.; Alexandratos, S.; Schleyer, P. v. R.; Streitwieser, A., Jr.; Schaefer, H. F., III, *J. Am. Chem. Soc.* **1978**, *100*, 5695–5700. (c) Böhm, M. C.; Gleiter, R.; Morgan, G. L.; Lusztyk, J.; Starowieyski, K. B. *J. Organomet. Chem.* **1980**, *194*, 257–263. (d) Marynick, D. S. *J. Am. Chem. Soc.* **1981**, *103*, 1328–1333.
(4) Most, but not all, MO calculations on beryllocene favor an η^5-η^1 ground-state structure. For pertinent references see: (a) Sundbom, M. *Acta Chem. Scand.* **1966**, *20*, 1608–1620. (b) Lopatko, O. Y.; Klimenko, N. M.; Dyatkina, M. E. *Zh. Strukt. Khim.* **1972**, *13*, 1128–1133. (c) Marynick, D. S. *J. Am. Chem. Soc.* **1977**, *99*, 1436–1441. (d) Chiu, N.-S.; Schäfer, L. *Ibid.* **1978**, *100*, 2604–2607. (e) Demuynck, J.; Rohmer, M. M. *Chem. Phys. Lett.* **1978**, *54*, 567–570. (f) Gleiter, R.; Böhm, M. C.; Haaland, A.; Johansen, R.; Lusztyk, J. *J. Organomet. Chem.* **1979**, *170*, 285–292 and ref 2a and 2b.
(5) Jutzi, P.; Kohl, F.; Hofmann, P.; Krüger, C.; Tsay, Y.-H. *Chem. Ber.* **1980**, *113*, 757–769.

0002-7863/82/1504-4064$01.25/0